WATER RESOURCES RESEARCH, VOL. 26, NO. 9, PAGES 2219–2227, SEPTEMBER 1990

Fourier Domain Shape Analysis Methods: A Brief Review and an Illustrative Application to Rainfall Area Evolution

PRAVEEN KUMAR AND EFI FOUFOULA-GEORGIOU

St. Anthony Falls Hydraulic Laboratory, Department of Civil and Mineral Engineering, University of Minnesota, Minneapolis

Morphological shape analysis techniques offer valuable tools for the study of several hydrologic and atmospheric processes. Detailed description of patterns, as well as evolution and comparison of patterns can be efficiently performed in the Fourier domain and by means of a finite number of Fourier descriptors. In this technical note we present a brief summary of three Fourier domain shape analysis methods: the complex plane method, the angular direction method, and the polar coordinates method. We illustrate the use of the complex plane method for studying the evolution of rainfall areas within a radar-depicted rainfall field for the purpose of short-term precipitation forecasting.

1. INTRODUCTION

Shape analysis deals with the extraction of a finite set of numerical features from a closed curve. These features should contain all essential information about the shape, so that they can be used to reconstruct the shape, to mathematically define and compute several of its geometrical properties, to discriminate among shapes, to classify a shape into one of a prespecified classes according to desired criteria, and to measure geometric similarity among different shapes. The need for description of irregular shapes and patterns arises often in hydrologic and atmospheric processes. For example, one may need to provide a concise but detailed morphological description of a pollutant concentration profile, of the shape of a drainage basin, or of the time-varying intensity profile of a storm. Traditionally, such geometries have been described in terms of a few representative parameters, such as area, perimeter, equivalent radius, and elongation ratio. It is believed that a more precise and mathematically based description of shapes would be beneficial in many hydrologic and atmospheric studies. The purpose of this paper is to introduce into the hydrological literature the ideas and methods of morphological shape analysis and present an example illustrating the potential of this theory to storm monitoring and short-term prediction.

There are two distinctly different classes of methods for obtaining numerical features from digital shapes. One class is based on encoding the boundary as a sequence of curved or linear segments and extracting features from these edges and contours. Two such methods are the chain encoding method [*Freeman*, 1970] and the polygonal approximation method [*Pavlidis and Ali*, 1975]. The second class of methods is based on a parametric description of the boundary curve of the shape. This function is then expanded in a Fourier series [e.g., *Cosgriff*, 1960] or in terms of other orthogonal functions such as Haar, Radamacher, or Walsh functions [*Beddow and Meloy*, 1980, p. 141]. The selection of one method versus another depends on the particular problems (e.g., see discussion of *Persoon and Fu* [1977]), the complexity of the profile, and the form of the original data describing the profile. In this paper only the second class of methods is considered, and in particular only three methods based on Fourier analysis are reviewed. Theoretical and experimental evidence suggests that Fourier domain–based methods result in efficient and useful descriptors [e.g., *Zahn and Roskies*, 1972] as compared to methods using other types of orthogonal functions.

The underlying idea of the Fourier domain analysis methods is the Fourier series representation of a parametric description of the boundary curve of interest. This frequency domain representation of a profile occurred to us recently as a convenient way of representing storm shapes, only to discover that it first appeared in the literature almost three decades ago (e.g., see *Cosgriff* [1960] for the earliest reference). It has since then been extensively studied in the electrical engineering/pattern recognition literature and also in the chemical engineering/material science literature. At this point of time, theoretical and applied research on morphological shape analysis is fairly advanced. This provides a solid background upon which developments and applications unique to hydrologic and atmospheric processes can be made. One such promising application, which is preliminarily studied here, is in short-term extrapolative precipitation forecasting where small-scale precipitation areas are extracted from the rainfall field and are subsequently monitored and forecasted [e.g., *Bohne*, 1988].

In this paper, three Fourier domain methods are reviewed: the complex plane method, the angular direction method, and the polar coordinates method. The first two methods are amenable to the analysis for any shape, whereas the third method is useful only for convex shapes. The review that follows is not exhaustive and is limited only to those theoretical elements which are deemed relevant and necessary for hydrologic and atmospheric applications. The reader is referred to the original references for further details. Under each method the discussion is organized as follows: first the parametric representation of the boundary curve is given together with its expansion in terms of Fourier descriptors (FDs). Then, the reconstruction of the shape from the FDs is discussed and several geometrical properties of the shape are derived in terms of the FDs. Finally, an application of the complex plane method to monitoring rainfall areas is presented for the purpose of short-term extrapolative precipitation forecasting.

Paper number 90WR00723.
0043-1397/90/90WR-00723$02.00

2. The Complex Plane Method

2.1. *Parametric Representation*

Let γ be a simple piecewise continuous closed curve in the complex plane. Using the normalized arc length $t = l/L$, $t \in [0, 1]$ as a parameter, the closed curve γ can be viewed as a continuous mapping from the unit interval onto the set of complex numbers, i.e.,

$$Z(t) = x(t) + iy(t) \qquad t \in [0, 1] \tag{1}$$

For convenience we assume that the curve γ has a counterclockwise (CCW) orientation, in the sense that as one moves along the boundary for increasing values of t, the interior of the region enclosed by the contour lies to the left. Notice that since the curve is closed, $Z(1) = Z(0)$ and $Z(t')$ for $t' \in [-\infty, \infty]$ is defined and is periodic with period unity, i.e., $Z(n + t) = Z(t)$, where $n \in I$, I being the set of integers and $t \in [0, 1]$. Hence, $Z(t)$ can be conveniently represented as a Fourier series

$$Z(t) = \sum_{k=-\infty}^{\infty} c_k e^{i2\pi kt} \tag{2}$$

where

$$c_k = \int_0^1 Z(t) e^{-i2\pi kt}\, dt \tag{3}$$

The piecewise continuity of $Z(t)$ assures the absolute convergence of the Fourier series at any point t and also the uniform convergence on any closed interval [e.g., *Voxman and Goetschel*, 1981, pp. 348–360].

Writing the complex coefficient c_k as $c_k = a_k e^{i\alpha_k}$, the real numbers a_k and α_k are the kth harmonic amplitude and phase angle, respectively. Hence,

$$x(t) = \sum_{k=-\infty}^{\infty} a_k \cos(2\pi kt + \alpha_k) \tag{4}$$

$$y(t) = \sum_{k=-\infty}^{\infty} a_k \sin(2\pi kt + \alpha_k) \tag{5}$$

2.2. *Calculating Fourier Descriptors for a Polygonal Curve*

In most practical applications the contour $Z(t)$ will be approximated by a piecewise continuous polygonal curve consisting of m line segments. *Persoon and Fu* [1977] have derived formulae for computing the Fourier coefficients c_k in case the curve γ is polygonal. These are repeated here for completeness.

Assume that γ has m vertices $V_0, \cdots, V_{m-1}$ and that V_0 is the starting point. Then,

$$c_k = \frac{1}{L(k2\pi/L)^2} \sum_{n=1}^{m} (b_{n-1} - b_n) \exp\left[-\left(\frac{ik2\pi l_n}{L}\right)\right] \tag{6}$$

where

$$l_n = \sum_{i=1}^{n} |V_i - V_{i-1}| \qquad n > 0,\ l_0 = 0 \tag{7}$$

$$b_n = \frac{V_{n+1} - V_n}{|V_{n+1} - V_n|}, \tag{8}$$

so $|b_n| = 1$. Having obtained c_k, the profile can be reproduced in detail by means of (2). Note that an infinite number of harmonics would reproduce the profile exactly and that a small finite number of harmonics would reproduce it only approximately. Error bounds associated with the truncated Fourier series can be found, for example, in the work by *Voxman and Goetschel* [1981, p. 633].

2.3. *Shape Properties of Interest*

Several shape properties of practical interest, such as orientation and aspect ratio, lose their physical meaning for shapes that are nonconvex and very irregular. Thus these properties are not defined under the general complex plane and angular direction methods. They are, however, extensively discussed under the polar coordinates method which applies to convex shapes only. Below, only expressions for three simple shape properties are given: area, equivalent, radius, and center of mass.

2.3.1. *Area.* Using Green's theorem the area enclosed within the closed contour $Z(t) = x(t) + iy(t)$ can be derived as

$$A = \frac{1}{2} \int_{t=0}^{1} [x(t)y'(t) - y(t)x'(t)]\, dt \tag{9}$$

which after substitution of the Fourier series expressions evaluates to

$$A = \sum_{k=-\infty}^{+\infty} |a_k|^2 k\pi \tag{10}$$

where $a_k = (c_k \bar{c}_k)^{1/2}$.

2.3.2. *Equivalent radius.* This is defined as the radius of a circle having the same area as that of the shape under consideration. Hence,

$$R_0 = \left(\sum_{k=-\infty}^{\infty} |a_k|^2 k \right)^{1/2} \tag{11}$$

2.3.3. *Center of mass.* The center of mass is given by

$$Z_c = \int_0^1 Z(t)\, dt = c_0 \tag{12}$$

where c_0 is the zeroth harmonic.

2.4. *Contour Similarity*

It is often necessary to compare two or more contours for classification purposes or for monitoring and quantitatively describing the shape evolution of a contour over time. Formal ways of such an analysis are presented below. First, contour similarity and the normalized form of a contour are defined. Then using these results, formal measures of distance between contours are presented.

The closed contour Z' is said to be similar to Z if the image of Z can be mapped onto the image of Z' by a sequence of translation, rotation, reflection, and change of scale operations. If $T = x_T + iy_T$ denotes the translation vector, K the scaling factor, α the angle of rotation about the origin, and t_0 the shift in the initial point, Z' is similar to Z if there exist real positive parameters t_0, α, K and a complex parameter T such that for all $t \in [0, 1]$ either

$$Z'(t) = K \exp(i\alpha) Z(t + t_0) + T \tag{13}$$

if there is no reflection, or

$$Z'(t) = K \exp(i\alpha) \overline{Z(-t - t_0)} + T \tag{14}$$

if there is a reflection about the x axis [*Richard and Hemami*, 1974]. The negative sign of t in (14) preserves the CCW sense of the curve for increasing t. This relation is an equivalence relation and may be used for classification of a set of curves into equivalence classes. It is easy to show that a reflection about a line $y = mx + d$ can be decomposed into a rotation by an angle β, where $\beta = \frac{1}{2} \tan^{-1} m$, and a translation by $T = 0 + id$.

If $\{c_k\}$ and $\{c'_k\}$ denote the Fourier coefficients for the contours Z and Z', respectively, the above two equations can be written in the form

$$c'_k = K \exp[i(\alpha + 2\pi k t_0)] c_k + \delta_{k,0} T \tag{15}$$

if there is no reflection, and

$$c'_k = K \exp[i(\alpha + 2\pi k t_0)] \overline{c_k} + \delta_{k,0} T \tag{16}$$

if there is reflection about the x axis [*Richard and Hemami*, 1974]. In the above equations, the indicator function $\delta_{k,0} = 1$ if $k = 0$ and $\delta_{k,0} = 0$ if $k \neq 0$.

2.5. *Canonical Form of a Contour*

The normalized form of a contour $Z(t)$ is given by

$$Z^*(t) = \frac{Z(t) - Z_c}{\|Z(t) - Z_c\|} \tag{17}$$

where Z_c is the centroid of the curve and

$$\|Z(t) - Z_c\|^2 = \int_0^1 |Z(t) - Z_c|^2 \, dt \tag{18}$$

Note that $Z^*(t)$ has zero mean (centroid at origin) and norm equal to unity. The normalized curve can be used as a representative/prototype of an equivalence class and hence defines the canonical form for that class.

It can be shown [*Richard and Hemami*, 1974] that the Fourier coefficients $\{c_k^*\}$ of the normalized curve $Z^*(t)$ are

$$c_k^* = c_k \left[\sum_{l=-\infty}^{+\infty} |c_l|^2 - |c_0|^2 \right]^{-1/2} \qquad k \neq 0 \tag{19}$$

2.6. *Measure of Distance Between Curves*

Richard and Hemami [1974] propose a measure of distance between two curves by finding the deviation of the correlation of the two normalized curves from unity, when the correlation is maximized by shifting the initial point (by τ^*), rotating (by β^*), and reflecting one normalized curve with respect to the other. They give the following expression for the distance $d(Z_1, Z_2)$ between curves Z_1 and Z_2

$$d(Z_1, Z_2) = \min(d_a, d_b) \tag{20}$$

where

$$d_a^2 = 2\left[1 - \max_{\tau} \left| \int_0^1 Z_1^*(t) \overline{Z_2^*(t + \tau)} \, dt \right| \right] \tag{21}$$

$$d_b^2 = 2\left[1 - \max_{\tau} \left| \int_0^1 Z_1^*(t) \overline{Z_2^*(-t - \tau)} \, dt \right| \right] \tag{22}$$

for $0 \leq \tau \leq 1$. The angle of rotation of one curve with respect to the other is given by

$$\beta^* = \arg \int_0^1 Z_1^*(t) \overline{Z_2^*(t + \tau^*)} \, dt \tag{23}$$

or

$$\beta^* = \arg \int_0^1 Z_1^*(t) \overline{Z_2^*(-t - \tau^*)} \, dt \tag{24}$$

for $0 \leq \beta^* < 2\pi$, where arg is the principal value of the angle of the complex number and τ^* is the point of maximization in equation (21) or (22).

If $\{c_{1,k}\}$ and $\{c_{2,k}\}$ denote the Fourier coefficients of the contours Z_1 and Z_2, respectively, and if the contours are represented by N-tuples over the field of complex numbers $Z = (z_1, z_2, \cdots, z_N)$, it can be shown that

$$d_a^2 = 2\left[1 - \max_j \left| \sum_{k=-n_1}^{n_2} c_{1,k}^* \overline{c_{2,k}^*} \exp\{-i2\pi kj/N\} \right| \right] \tag{25}$$

$$d_b^2 = 2\left[1 - \max_j \left| \sum_{k=-n_1}^{n_2} c_{1,k}^* c_{2,k}^* \exp\{-i2\pi kj/N\} \right| \right] \tag{26}$$

with $n_1 + n_2 + 1 = N$. The maximization in the above equation is easily obtained by taking the fast Fourier transform (FFT) of the products $c_{1,k}^* \overline{c_{2,k}}^*$ and $c_{1,k}^* c_{2,k}^*$ and finding the jth component with the largest magnitude. This procedure has been implemented in the example presented in a later section.

Note that two curves are similar when $d(Z_1, Z_2) = 0$, i.e., when the maximized correlation between the two curves is unity. If $d_a = 0$, Z_2 fits Z_1; if $d_b = 0$, Z_2 fits the reflection of Z_1. Also note that the rotation, scale, and translation parameters in (13) or (14) are recoverable from

$$\alpha = \beta^* \tag{27}$$

$$K = \frac{\|Z_1 - Z_{c1}\|}{\|Z_2 - Z_{c2}\|} \tag{28}$$

$$T = Z_{c1} - Ke^{i\alpha} Z_{c2} \tag{29}$$

For an alternate method of obtaining distance between curves see *Persoon and Fu* [1977].

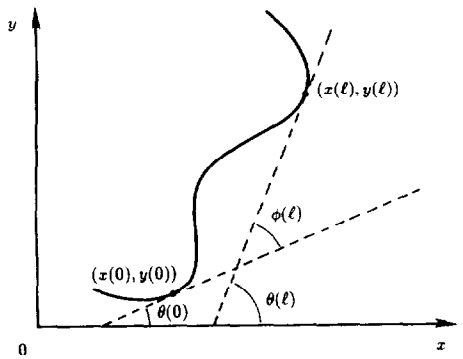

Fig. 1. Parametric representation of a curve with the angular direction method.

3. The Angular Direction Method

3.1. *Parametric Representation*

Assume again that γ is a counterclockwise oriented simple closed curve with parametric representation $(z(l) = (x(l), y(l))$ where l is the arc length and $0 \le l \le L$. Following *Zahn and Roskies* [1972], denote the angular direction of γ at point l by the function $\theta(l)$ and let $\theta_0 = \theta(0)$ be the absolute angular direction at the starting point $Z(0)$. Define the cumulative angular function $\phi(l)$ as the net amount of angular bend between starting point and point l (see Figure 1). With this definition $\phi(l) = \theta(l) - \theta(0)$ except for possible multiples of 2π. Note that $\phi(0) = 0$ and $\phi(L) = 2\pi$ because all smooth simple closed curves with CCW orientation have a net angular bend of 2π. Also note that if the curve γ winds in a spiral then $|\phi(l)|$ can achieve values larger than 2π. The domain of definition $[0, L]$ of $\phi(l)$ contains absolute size information and one would like to normalize to the interval $[0, 2\pi]$ which is standard for periodic functions. Hence we define a normalized variant $\phi^*(t)$ as

$$\phi^*(t) = \phi(Lt/2\pi) - t \tag{30}$$

where $t = 2\pi l/L$ ranges from 0 to 2π. (We draw the attention of the reader to the fact that our expressions differ from those of Zahn and Roskies who consider clockwise oriented curves). Note that $\phi^*(t) \equiv 0$ for a circle and that $\phi^*(t)$ is invariant under translation, rotation, and scaling, i.e., changes of the perimeter L. With the above definitions, it is apparent that two curves with same starting points and identical shapes (i.e., curves that differ only by a combination of translation, rotation, and change in size) map into the same function ϕ^*.

Expanding $\phi^*(t)$ as a Fourier series

$$\phi^*(t) = \mu_0 + \sum_{k=1}^{\infty} (a_k \cos kt + b_k \sin kt) \tag{31}$$

where

$$\mu_0 = \frac{1}{2\pi} \int_0^{2\pi} \phi^*(t)\, dt \tag{32}$$

$$a_k = \frac{1}{\pi} \int_0^{2\pi} \phi^*(t) \cos kt\, dt \tag{33}$$

$$b_k = \frac{1}{\pi} \int_0^{2\pi} \phi^*(t) \sin kt\, dt \tag{34}$$

Note that the Fourier coefficients (a_k, b_k) contain no information relating to the absolute position or rotational orientation of the curve. On the other hand (since $\phi^*(0) = 0$)

$$\mu_0 = -\sum_{k=1}^{\infty} a_k \tag{35}$$

and therefore μ_0 carries information related to the particular starting point used.

An equivalent expansion of $\phi^*(t)$ in terms of amplitude and phase angle is

$$\phi^*(t) = \mu_0 + \sum_{k=1}^{\infty} A_k \cos (kt - \alpha_k) \tag{36}$$

where (A_k, α_k) are polar coordinates of the point (a_k, b_k). Note that the harmonic amplitudes $\{A_k\}$ are invariant under translations, rotations, changes in size, and shifts in the starting point, whereas the phase angles $\{\alpha_k\}$ are only affected by shifts in the starting point.

3.2. *Calculating Fourier Descriptors for a Polygonal Curve*

Zahn and Roskies [1972] have derived formulae for the Fourier coefficients $\{a_k, b_k\}$ and μ_0 when γ is a polygonal curve. These formulae are repeated here for easy reference.

Assume that γ has m vertices $V_0, \cdots, V_{m-1}$ and that the edge (V_{i-1}, V_i) has length δl_i. The change in angular direction at vertex V_i is $\delta\phi_i$ and $L = \Sigma_{i=1}^{m} \delta l_i$. With these definitions

$$\phi(l) = \sum_{i=1}^{n} \delta\phi_i \qquad \sum_{i=1}^{n} \delta l_i \le l < \sum_{i=1}^{n+1} \delta l_i \tag{37}$$

$$\phi(l) = 0 \qquad 0 \le l < \delta l_1 \tag{38}$$

Using the definitions of μ_0, a_k, b_k (equations (32), (33), and (34)) and the definition of $\phi^*(t)$ (equation (30)) and after lengthy calculations one can obtain [see *Zahn and Roskies*, 1972]

$$\mu_0 = -\pi + \frac{1}{L} \sum_{j=1}^{m} l_j \delta\phi_j \tag{39}$$

$$a_k = +\frac{1}{k\pi} \sum_{j=1}^{m} \delta\phi_j \sin \frac{2\pi k l_j}{L} \tag{40}$$

$$b_k = -\frac{1}{k\pi} \sum_{j=1}^{m} \delta\phi_j \cos \frac{2\pi k l_j}{L} \tag{41}$$

where $l_j = \Sigma_{i=1}^{j} \delta l_i$.

3.3. *Reconstruction of a Curve Using Fourier Descriptors*

If curve γ is described by $\theta(l)$ and starting point $Z(0)$, the position of point $Z(l)$ is given from the reconstruction theorem [*Zahn and Roskies*, 1972]

$$Z(l) = Z(0) + \int_0^l e^{i\theta(\lambda)}\, d\lambda \tag{42}$$

which is equivalent to

$$x(l) = x(0) + \int_0^l \cos\,\theta(\lambda)\, d\lambda \tag{43}$$

$$y(l) = y(0) + \int_0^l \sin\,\theta(\lambda)\, d\lambda \tag{44}$$

Using the reconstruction theorem and a truncated Fourier series expansion of $\phi^*(l)$ one can derive the following practical formula for curve reconstruction based on the Fourier descriptors $\{A_k, \alpha_k\}_{k=1}^N$ and the triplet $(L, \theta_0, Z(0))$ giving length, initial tangential direction, and position of starting point, respectively:

$$Z(l) = Z(0) + \frac{L}{2\pi}\int_{t=0}^{2\pi l/L} \exp\left\{i\left[t + \theta_0 + \mu_0 + \sum_{k=1}^{N} A_k \cos\,(kt - \alpha_k)\right]\right\} dt \tag{45}$$

Note here that μ_0 is not a free variable but is given by $\{A_k, \alpha_k\}_{k=1}^N$ as $\mu_0 = \sum_{k=1}^N A_k \cos\,\alpha_k$. Observe that if one desires a curve of similar shape but with starting point $\bar{Z}(0)$, initial direction $\bar{\theta}_0$, and total arc length $\bar{L}$ the same formula is used but with these values instead of $Z(0)$, θ_0, and L.

From the above formula one directly obtains

$$x(l) = x(0) + \frac{L}{2\pi}\int_{t=0}^{2\pi l/L} \cos\left\{t + \theta_0 + \mu_0 + \sum_{k=1}^{\infty} A_k \cos\,(kt - \alpha_k)\right\} dt \tag{46}$$

$$y(l) = y(0) + \frac{L}{2\pi}\int_{t=0}^{2\pi l/L} \sin\left\{t + \theta_0 + \mu_0 + \sum_{k=1}^{\infty} A_k \cos\,(kt - \alpha_k)\right\} dt \tag{47}$$

It should be noted that not all curves described by equation (45) are closed. *Zahn and Roskies* [1972] provide conditions under which closure is ensured. They also provide relationships between the Fourier descriptors of two curves γ and γ' when γ' results from γ by a geometric transformation, i.e., scaling, reflection, rotation, or using a different starting point.

4. THE POLAR COORDINATES METHOD

4.1. *Parametric Representation*

Let γ again be a counterclockwise oriented simple closed curve with parametric representation $R(\theta)$, where (R, θ) are the polar coordinates of a point on the curve with respect to an arbitrary coordinate system centered in the curve's interior. $R(\theta)$ is a periodic function with period 2π and therefore can be expressed in terms of a Fourier series of the form

$$R(\theta) = a_0 + \sum_{n=1}^{\infty} (a_n \cos\,n\theta + b_n \sin\,n\theta) \tag{48}$$

where a_n and b_n are the Fourier coefficients corresponding to the nth harmonic. Note that the polar coordinate method is appropriate for convex shapes only since for nonconvex (i.e., reentrant) shapes, at certain values of θ there is more than one value of $R(\theta)$.

4.2. *Shape Properties of Interest*

In this section, the following descriptive properties of a geometrical shape are studied: area, center of mass, orientation, moments of inertia and higher area moments, aspect ratio, equivalent radius, and statistical properties of the radius $R(\theta)$ such as the mean, second, and third central moments. These properties are first defined and expressions are given in terms of cartesian (x, y) and polar (R, θ) coordinates of the profile, as well as in terms of the Fourier coefficients, whenever such expressions are derivable.

4.2.1. *Area.*

$$A = \int_y \int_x dx\, dy = \int_{\theta=0}^{2\pi} \int_{r=0}^{R(\theta)} r\, dr\, d\theta \tag{49}$$

Using Parseval's theorem [e.g., *Carslaw*, 1950, p. 285] the expression of the area in terms of the Fourier coefficients can be shown to be

$$A = \pi\left\{a_0^2 + \frac{1}{2}\sum_{n=1}^{\infty}(a_n^2 + b_n^2)\right\} \tag{50}$$

4.2.2. *Center of Mass.* The cartesian coordinates (x_c, y_c) of the center of mass are given by

$$x_c = \frac{1}{A}\int\int_A x\, dx\, dy = \frac{1}{2A}\int_{\theta=0}^{2\pi}\int_{r=0}^{R(\theta)} r\cos\,\theta\; r\, dr\, d\theta = \frac{1}{3A}\int_{\theta=0}^{2\pi} R^3(\theta)\cos\,\theta\, d\theta \tag{51}$$

Similar expressions hold for y_c.

4.2.3. *Orientation.* We define orientation here by the angle ϕ_0 (measured from the $\theta = 0$ axis in a counterclockwise direction), where ϕ_0 is solution of the equation $\partial f/\partial\phi = 0$ under the condition $\partial^2 f/\partial\phi^2 > 0$, where

$$f = \int\int_A (x \sin\phi + y \cos\phi)^2 \, dx \, dy \tag{52}$$

$$= \int_{\theta=0}^{2\pi} \int_{r=0}^{R(\theta)} r^2 \sin^2(\theta - \phi) r \, dr \, d\theta$$

$$= \frac{1}{4} \int_{\theta=0}^{2\pi} R^4(\theta) \sin^2(\theta - \phi) \, d\theta \tag{53}$$

Note that the axis defined by the orientation ϕ_0 can be interpreted as the axis about which the moment of inertia is minimum.

4.2.4. *Area moments.* The kth area moment about the x axis is

$$M_{k,x} = \int\int_A y^k \, dx \, dy = \frac{1}{k+2} \int_{\theta=0}^{2\pi} R^{k+2}(\theta) \sin^k \theta \, d\theta \tag{54}$$

and a similar expression holds for $M_{k,y}$. Of special interest are the second moments or moments of inertia.

4.2.5. *Aspect ratio.* We define the aspect ratio (AR) here as the ratio of the length of the line passing through the center of mass and parallel to orientation over the length of the line passing through the center of mass and perpendicular to orientation

$$AR = \frac{R(\phi_0) + R(\phi_0 + \pi)}{R[\phi_0 + (\pi/2)] + R[\phi_0 + (3\pi/2)]} \tag{55}$$

Defining $R'(\theta) = R(\phi_0 + \theta)$ and expanding $R'(\theta)$ in Fourier series with Fourier coefficients $\{a_n', b_n'\}_{n=1}^N$, the AR can be written in the form

$$AR = \frac{a_0' + \sum_{n=1}^{N/2} a_{2n}'}{a_0' + \sum_{n=1}^{N/2} (-1)^n a_{2n}'} \tag{56}$$

using a result of *Beddow and Meloy* [1980, p. 37]. Note that the Fourier coefficients $\{a_n', b_n'\}$ are obtained from the corresponding coefficients $\{a_n, b_n\}$ via the transformation

$$[a_n' \quad b_n'] = [a_n \quad b_n] \begin{bmatrix} \cos n\phi_0 & -\sin n\phi_0 \\ \sin n\phi_0 & \cos n\phi_0 \end{bmatrix} \tag{57}$$

This transformation is analogous to that for a change in coordinate system by rotation about the origin.

4.2.6. *Equivalent radius.* This is defined as the radius of a circle having the same area as that of the shape. Hence,

$$R_0 = \left[a_0^2 + \frac{1}{2} \sum_{n=1}^{\infty} (a_n^2 + b_n^2) \right]^{1/2} \tag{58}$$

4.2.7. *Statistical moments of $R(\theta)$.* The first three statistical moments of $R(\theta)$ are expressible in terms of the Fourier coefficients. These expressions can be found in the work by *Luerkens et al.* [1982] and are repeated here for easy reference.

$$\mu_1 = E[R(\theta)] = a_0 \tag{59}$$

$$\mu_2 = E[(R(\theta) - a_0)^2] = \frac{1}{2} \sum_{n=1}^{\infty} (a_n^2 + b_n^2) \tag{60}$$

$$\mu_3 = E[(R(\theta) - a_0)^3] = \frac{3}{4} \sum_{m=1}^{\infty} \sum_{n=1}^{\infty} [a_m a_n a_{m+n} - b_m b_n a_{n+m} + a_m b_n b_{n+m} + b_m a_n b_{m+n}] \tag{61}$$

It should be noted that the above measures of geometry are not invariant under geometrical transformations such as translation, scaling, rotation, and reflection, and therefore cannot be used for shape comparison and classification. The reader is referred to *Luerkens et al.* [1982] for derivation of certain geometrically invariant shape descriptors.

5. Comparison of Methods

The relative merits of the three methods described above can be best studied in the light of the following criteria: representational convenience, reconstruction efficiency, derivation of geometrical properties, derivation of transformation invariant properties, and classification of shapes.

The complex plane method and the angular direction method are useful for any kind of shape whereas the polar coordinate method can be used only for convex shapes. The complex plane method presents advantages over the angular direction method in both representation and reconstructional efficiency since x and y are more natural coordinates both in terms of measurement considerations and conceptual understanding as compared to the angular direction ϕ and arc length l. As is evident from (46) and (47), the curve reconstruction in the angular direction method involves an integration over an infinite sum which can be of concern from the computational efficiency standpoint. Moreover, most of the geometrical properties have to be evaluated numerically in both of these methods, closed form expressions being unavailable. Both the complex plane method and the angular direction method present very useful analytical tools for the representation of transformation invariant properties and for comparison and classification of shapes. However, the complex plane method is definitely more efficient since (25) and (26) present an extremely powerful and efficient tool for curve matching and (19) can be used to find the Fourier coefficients of a normalized curve. An analogous tool in the angular direction method is not available although *Zahn and Roskies* [1972] have discussed an alternate method for curve matching.

The polar coordinate method, whenever it can be used, presents certain specific advantages over the other two methods as it enables the direct definition of certain useful shape properties such as orientation and aspect ratio. Besides, closed form solutions are available for most of the transformation invariant properties which makes the method accessible for classification and curve matching.

6. Monitoring and Short-Term Forecasting of Precipitation Fields

Short-term precipitation forecasting (10 min up to 1 to 2 hours and spatial resolution of a few kilometers) can be accomplished by monitoring the motion, shape, size, and

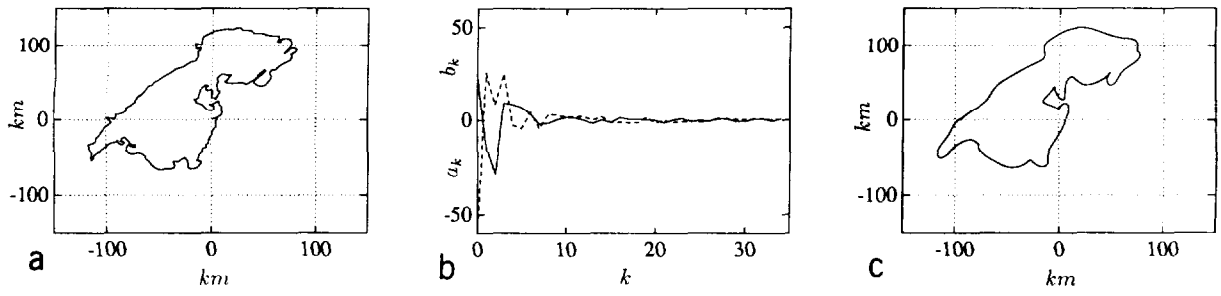

Fig. 2. Frame 23 (hour 1616 to 1716 LT). (*a*) Precipitation area enclosed within the contour of 4 mm/h (from the original radar data; distances are in kilometers related to radar location). (*b*) Fourier coefficients $a_k = Re\ (c_k)$ (solid line) and $b_k = Im\ (c_k)$ (dashed line). (*c*) Reconstructed form of the contour from 35 harmonics.

intensity of small-scale precipitation areas within a precipitation field and extrapolating their trends in space and time. This type of observation-driven extrapolative forecasting methodology has been the topic of several previous investigations [e.g., *Bellon and Austin*, 1976] and is currently enjoying renewed interest [e.g., *Bohne* 1988; *Browing and Collier*, 1989]. Past efforts on extrapolative forecasting have concentrated on advection or cross-correlation methods which basically translate the whole precipitation field. Current research is directed toward methods that can account for evolution of small-scale precipitation areas within the rainfall field of interest. Under these methods, feature areas are extracted by thresholding the data with selected intensity levels, thus forming a series of areas enclosed within contour boundaries. These areas are then monitored and forecasted.

One of the most important steps in such an extrapolative forecasting methodology is feature representation. *Bohne* [1988] describes two methodologies for feature description, namely segmentation methods and whole contour methods and discusses their advantages and disadvantages. Current trend leans toward the whole contour methods, such as the Fourier domain feature representation methods discussed in this paper, which although more computationally intensive are more amenable to automation and allow for interesting interpretations. We believe that these methods, which have not yet been extensively explored, offer a promising alternative worthy of further investigation.

In this section, an implementation of the complex plane method to the quantitative description and monitoring of precipitation patterns depicted by a radar is given. The storm analyzed is a squall line which occurred over central Oklahoma on May 27, 1987. It lasted for approximately 8 hours (1130 to 1930 LT) and deposited a maximum point rainfall in excess of 230 mm. The total area covered by nonzero rainfall varied from 90,000 to 112,000 km^2. This storm was monitored by the National Severe Storm Laboratory (NSSL) WSR-57 radar which is a 10-cm-wavelength system with a peak power of 305 kW and a beam width of 2.2°. The conversion of the cloud reflectivity factor (at four elevations) to rainfall rates was done at the NSSL in Norman, Oklahoma, using their standard conversion procedures which include adjustments for ground clutter (Tim O'Bannon, personal communication, 1989). The data provided to us were rainfall rates (in millimeters per hour) averaged over one hour intervals lagged by approximately 5–10 min from each other. Each hourly rainfall pattern will be referred to as a frame, i.e., average rate over the time period 1131 to 1231 LT will be called frame 1; 1140 to 1240 LT frame 2; up to the last frame number 36 which is the accumulation over the last hour of 1822 to 1922 LT. The rainfall data were provided in polar coordinates over angular increments of one degree (from 0 to 2π counterclockwise) and with 115 values per degree at every 2 km radial distance covering the 230 km radius of the radar field.

In this example implementation we have concentrated on a mesoscale rainfall area enclosed within the contour of 4 mm/h and we have followed its evolution over the duration of the storm. The 4 mm/h contour level was selected arbitrarily but the procedure would be the same had another cutoff level been selected. During the first hour of the storm there were three distinct rainfall areas enclosed within contours of 4 mm/h and having areal extent exceeding 1,000 km^2. The areal extents of these areas were approximately 10,000 km^2, 1,200 km^2, and 2,100 km^2. These rainfall areas kept their identity for the first 45 min and then some merged with each other. This merging can be easily observed in the Fourier domain due to abrupt changes in the Fourier descriptors. Here we only report the results of the evolution of the largest and most well defined of these rainfall areas during the time period of 1448 to 1800 LT. The shape of this precipitation area did not change much over the studied period of time. It is shown here only for two frames, frames 23 (hour 1616 to 1716 LT) and 24 (hour 1625 to 1725 LT) where the most abrupt change in shape took place (see Figures 2*a* and 3*a*).

Cartesian coordinates (with respect to a system centered at the center of the radar and having the positive direction of the horizontal and vertical axes in the east and north directions, respectively) of the boundary of the rainfall areas of interest were extracted from the original polar coordinate data using a contouring algorithm and specifying the cutoff contour level of 4 mm/h. In order to be able to use efficient FFT algorithms, a new array of cartesian coordinates was formed from the original one by cubic spline interpolation. The new array had a size of integral power of two (here 256 values were used) and had points uniformly spaced on the total arc length. The Fourier series coefficients were computed via FFT. The first 35 Fourier coefficients $a_k = Re\ (c_k)$ (solid line) and $b_k = Im\ (c_k)$ (dashed line) are displayed in Figures 2*b* and 3*b* for frames 23 and 24, respectively. These coefficients were used to produce the reconstructed profiles shown in Figures 2*c* and 3*c*. Note that the zeroth harmonic corresponds to the centroid of the profile as can be verified from the position of the original intensity contours.

In order to quantify the changes in the shape of the rainfall area as it evolves, the distance measure between successive

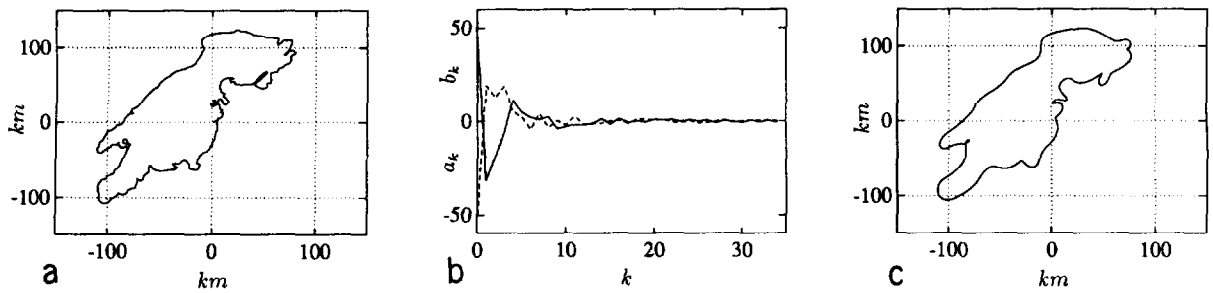

Fig. 3. Same as Figure 2 for frame 24 (hour 1625 to 1725 LT).

contours was computed as explained in section 2.6. For that, the normalized forms of the contours were found (that is the forms with centroid centered at the origin and having norm equal to unity). Figure 4*a* shows the distance $d(Z_{i-1}, Z_i)$ between contours Z_{i-1} and Z_i versus frame number i. It is interesting to observe that this measure faithfully reproduces the qualitative observation that the most abrupt change in shape occurred between frames 23 and 24. Figure 4*b* shows the angle β^* (in degrees) versus frame number. Recall that this is the rotation angle needed to obtain maximum correlation between successive frames and therefore provides another measure of change. As was expected, this angle is very small for a squall line development since during the studied period there is hardly any change in the orientation of the storm system. Figure 4*c* shows the scale factor K, where $Z_{i-1} = KZ_i$, versus frame number. K^2 measures the relative change in the size of the area enclosed within successive contours, and as expected the most drastic change occurs between frames 23 and 24. It is interesting to note that the distance d between the intensity contour of the first (frame 14) and the last studied frame (number 28) is 0.499 indicating the drastic overall difference between the shape of rainfall intensity contours at the beginning and end of the studied period. Also, the overall rotation angle β^* is 9.816°, and K is 0.945 implying a strong change in orientation and a negligible change in areal extent of this precipitation area over the studied period of two hours.

The example presented above was mainly illustrative of the ability of these methods to quantitatively describe a shape and measure changes in shape and size of tracked figures. More extensive research is needed to fully explore the potential of the Fourier domain shape analysis methods for the quantitative description of the storm evolution process and short-term precipitation forecasting. First, the problem of deciding what feature areas should be extracted and monitored from the precipitation field, i.e. what intensity cutoff levels to use for feature definition, requires further study. This issue is currently under investigation by the authors [*Foufoula-Georgiou and Kumar*, 1989]. Second, problems arising with merging and splitting of rainfall areas and the automatic tracking of individual entities, especially at smaller spatial scales such as rain cells, need special attention. Fortunately, such abrupt changes in the rainfall field are reflected in the Fourier descriptors of the individual entities and the potential of these methods should be explored toward this end. Nevertheless, by visual inspection of the radar data and understanding of the meteorological conditions of the storm, a semiautomatic approach is always feasible and becomes especially efficient when used simultaneously with shape analysis methods.

7. Summary and Conclusions

The study of shape properties is of special interest in several hydrologic and atmospheric processes. For example, it is often desirable to preserve the total area contaminated with a pollutant or covered by a storm; the center of mass of a catchment is often related to the distance from the outlet along the main channel and is often used as an explanatory variable of hydrograph parameters; the orientation of a storm may provide an accurate descriptor of the direction of storm movement; and the aspect ratio may provide a simple descriptor of the stage of storm evolution (initiation, maturity, dissipation) or may be related to physiographical properties of a drainage basin, as for example, catchment relief. Also, the statistical moments of the radius of the shape are useful in assessing, for example, the mean and variability of the extent of a storm or a pollutant spill.

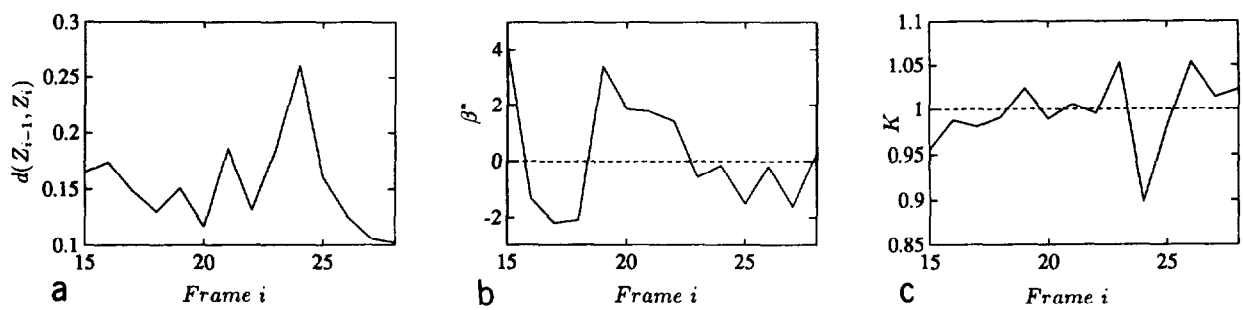

Fig. 4. (*a*) Distance $d(Z_{i-1}, Z_i)$ between contours Z_{i-1} and Z_i for successive frames versus frame number. (*b*) Angle of rotation β^* (degrees) between contours of successive frames versus frame number. (*c*) Scaling factor K between contours of successive frames versus frame number.

Frequency domain shape analysis provides convenient mathematical tools for studying these properties. In this paper, an attempt is made to illustrate the advantages of the Fourier domain shape analysis methods, which lend considerable ease in evaluation of certain geometrical properties, and provide the tools for rigorous comparison, classification, and study of shapes. The three methods reviewed here, i.e., the complex plane method, the angular direction method, and the polar coordinates method, have relative merits and the choice of a particular method depends on the shape under consideration, the form in which data are available, and the particular interest of the analyst. However, we believe that the complex plane method, applicable to any kind of shape, is more versatile and is also computationally efficient. A promising application of the complex plane method is in short-term extrapolative precipitation forecasting where feature areas extracted from a precipitation field are described in terms of a finite set of Fourier shape descriptors. Thus the problem of precipitation forecasting ultimately results in extracting and forecasting a set of shape descriptors. An illustrative example of the implementation of the complex plane method to the problem of rainfall area monitoring for short-term precipitation forecasting has been presented.

Acknowledgments. This research was supported by the National Science Foundation under grants CES-8708825 and BSC-8957469. The authors thank Tim O'Bannon of the NEXRAD Operational Support Facility, Norman, Oklahoma, for helpful discussions and for providing the radar data.

REFERENCES

Beddow, J. K., and T. P. Meloy, *Advanced Particulate Morphology*, CRC Press, Boca Raton, Fla., 1980.

Bellon, D. E., and G. L. Austin, SHARP (short-term automated radar prediction): A real time test, in *17th Conference on Radar Meteorology*, pp. 522–525, American Meteorological Society, Boston, Mass., 1976.

Bohne, A. R., Extrapolative forecasting of precipitation and cloud fields, paper presented at the Conference on Mesoscale Precipitation: Analysis, Simulation and Forecasting, Mass. Inst. of Technol., Boston, Mass., 1988.

Browing, K. A., and C. G. Collier, Nowcasting of precipitation systems, *Rev. Geophys.*, *27*(3), 345–370, 1989.

Carslaw, H. S., *An Introduction to the Theory of Fourier Series and Integrals*, 3rd ed., Dover, New York, 1950.

Cosgriff, R. L., Identification of shapes, *Rep. 820-11*, Ohio State Univ. Res. Foundation, Columbus, Dec. 1960.

Foufoula-Georgiou, E., and P. Kumar, Identification of natural scales from a radar depicted rainfall field for model building and parameter estimation, *Eos Trans. AGU*, *70*, 1085, 1989.

Freeman, H., Boundary encoding and processing, in *Picture Processing and Psychopictorics*, edited by B. S. Lipkin and A. Rosenfeld, pp. 241–306, Academic, San Diego, Calif., 1970.

Luerkens, D. W., J. K. Beddow, and A. F. Vetter, Morphological Fourier descriptors, *Powder Technol.*, *31*, 209–215, 1982.

Pavlidis, T., and F. Ali, Computer recognition of handwritten numerals by polygonal approximation, *IEEE Trans. Syst. Man Cybern.*, *SMC-6*, 610–614, 1975.

Persoon, E., and K.-S. Fu, Shape discrimination using Fourier descriptors, *IEEE Trans. Syst. Man Cybern.*, *SCM-7*, 170–179, 1977.

Richard, C. W., and H. Hemami, Identification of three dimensional objects using Fourier descriptors of the boundary curve, *IEEE Trans. Syst. Man Cybern.*, *SMC-4*, 371–378, 1974.

Voxman, W. L., and R. H. Goetschel, Jr., *Advanced Calculus: An Introduction to Modern Analysis*, Marcel Dekker, New York, 1981.

Zahn, T. C., and R. Z. Roskies, Fourier descriptors for plane closed curves, *IEEE Trans. Comput.*, *C-21*, 269–281, 1972.

E. Foufoula-Georgiou and P. Kumar, St. Anthony Falls Hydraulic Laboratory, Mississippi River and 3rd Avenue SE, University of Minnesota, Minneapolis, MN 55414.

(Received January 11, 1990;
accepted March 20, 1990.)